Morphology Control of Binary Polymer Mixtures by Spinodal Decomposition and Crystallization. 1. Principle of Method and Preliminary Results on PP/EPR†

Nobuyuki Inaba, Kazuo Sato, and Shyunichi Suzuki

Polymer Research Laboratory, Idemitsu Petrochemical Co. Ltd., Anegasaki, Ichihara City, Chiba, 299-01, Japan

Takeji Hashimoto*

Department of Polymer Chemistry, Kyoto University, Kyoto 606, Japan.
Received December 12, 1985

ABSTRACT: A method to control morphology of binary mixtures of polymers in which at least one constituent is crystallizable was explored by using polypropylene (PP) and ethylene–propylene random copolymer (EPR) mixtures as model systems. The method involves demixing above the melting temperatures of the constituent polymers according to spinodal decomposition, to the extent desired for particular purposes, and subsequent crystallization from the demixed system. Rapid crystallization from the demixed system was found to exhibit the morphology of space-filling spherulites, containing "structure memory" of the liquid–liquid phase separation of PP and EPR that resulted from the spinodal decomposition and subsequent coarsening processes occurring before the crystallization. The structure memory is a periodic spatial concentration fluctuation with a wavelength Λ_m that can be controlled by the time allowed for the isothermal demixing process. For the rapid crystallization process, crystallization takes place and proceeds in and through PP-rich domains without invoking long-range rearrangement of PP molecules such as segregation of the EPR component from crystallizing fronts of PP, very similar to the process of "solidification" proposed by Fischer et al. (i.e., a solidification in PP-rich domains with continuous and periodic spatial arrangements). In the case that Λ_m is smaller than the average diameter D_{sp} of the spherulites, the spherulites contain the structure memory as their internal structures.

I. Introduction

Demixing mechanisms and kinetics of polymer mixtures in the liquid state are current research topics attracting many researchers from both academic and industrial institutions. From a scientific viewpoint the study involves a fundamental problem of self-organization in nonequilibrium systems[1] of polymers. From an industrial viewpoint it involves exploitation of methods to control the supermolecular structures at various spatial levels and at various depths of demixing in terms of magnitude of the concentration fluctuations, which, it is hoped, will result in control of physical properties of the materials.

In this paper we deal with binary mixtures of polypropylene (PP) and ethylene–propylene random copolymer (EPR). The two particular polymers PP and EPR used in this studies are highly immiscible. Consequently they invariably involve demixing in the liquid state above the melting temperatures (T_m) of the constituent polymers.[2] The demixing occurs at all temperatures where the polymers do not thermally degrade.[3-7] The system above the T_m's will first be demixed to various stages by spinodal decomposition[2-16] and subsequent coarsening processes[17-29] and then crystallized by rapidly quenching the mixture in ice water. By using this method of solidification, we can observe the interplay of the two kinds of phase separation or transition, i.e., liquid–liquid (L–L) phase separation above T_m and liquid–solid transition (or crystallization) below T_m, in controlling the morphology of the mixture.

Demixing in the molten state causes spatially periodic concentration fluctuations that originate from spinodal decomposition and its subsequent coarsening, and these in turn cause spatial variations of melting temperature and rate of crystallization of the PP constituent. It will be shown that this memory of L–L demixing is maintained during the rapid crystallization process and locked in the volume-filling spherulites. The "content of the memory" will be shown to be controllable by demixing in the molten state and also by crystallization. Detailed kinetic studies of the spinodal decompoition in early and late stages of this mixture are beyond the scope of the present paper and will be described elsewhere.[2]

II. Experimental Section

1. Specimens: PP and EPR. The PP is isotactic polypropylene with a weight-average molecular weight M_w of 2.35×10^5 and a heterogeneity index $M_w/M_n = 4.1$ as measured by GPC. M_n being the number-average molecular weight. The EPR used in this work contains 73 mol % ethylene and has $M_w = 1.49 \times 10^5$ and $M_w/M_n = 2.5$. The EPR shows a small amount of crystallinity when annealed for a long period of time under conditions favorable for crystallization, but the presence of this small crystallinity is unimportant for this work.

2. Sample Preparation. A mixture of PP and EPR with 50/50% (w/w) was dissolved to a dilute solution in hot xylene. The solution was poured into a large amount of methanol cooled with ice. The precipitate containing a mixture of PP and EPR was cold pressed into thin-film specimens. The films thus prepared were designated Q and used as starting film specimens.[38]

3. Experimental Technique. Structure evolution in the mixture both above and below T_m of PP was observed by polarized (V_V) and depolarized light scattering (H_V). The scattering apparatus is schematically described in Figure 1. A plane-polarized laser beam (He–Ne laser, 20 mW, $\lambda_0 = 6320$ Å) was the incident source. The polarization direction of the beam was varied by a polarization rotator that contains a half-wave retardation plates as its essential part. The sample was placed on a Mettler hot stage mounted on a horizontal XY stage. The scattered light intensity was recorded through an analyzer onto Polaroid Land Pack films or by a CCD video camera connected to a dynamic image analyzer (DIA). The DIA can convert the input image of the camera into a 512 × 512 digital data array at a video rate of $^1/_{30}$ s with interlacing mode and $^1/_{60}$ s with noninterlacing mode, by using an 8-bit video analog-to-digital converter. The digitized image is accumulated in the frame accumulator which consists of 512 × 512 words of 16-bit wide memory. The details of the DIA–camera system for the high-speed time-resolved light scattering will be presented elsewhere.[30,31]

† Presented in part before the 34th Polymer Symposium, the Society of Polymer Science, Japan, Sept 26–28, 1985. Inaba, N.; Sato, K.; Suzuki, S.; Hashimoto, T. *Polym. Prepr., Jpn., Soc. Polym. Sci., Jpn.*, **1985**, *34*, 2809.

0024-9297/86/2219-1690$01.50/0

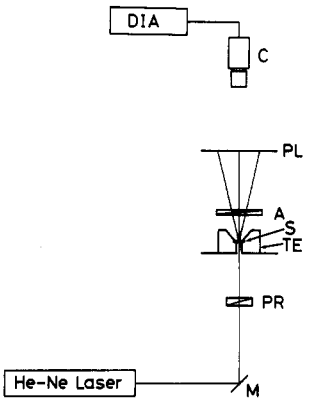

Figure 1. Time-resolved light scattering apparatus used in this work: M, mirror; PR, polarization rotator; TE, temperature enclosure (Mettler hot stage); S, sample; A, analyzer; PL, Polaroid Land film holder or screen; C, CCD camera, DIA, dynamic image analyzer.

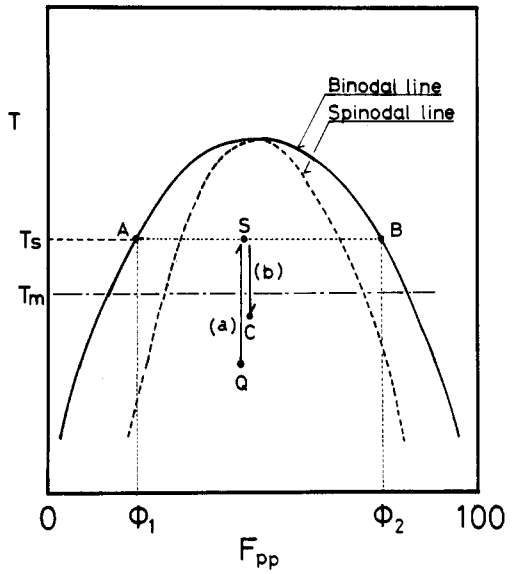

Figure 2. Schematic diagram showing a thermal history employed in this study for morphological control by spinodal decomposition and crystallization: Q, starting specimens; T_m, melting temperature of PP at a given composition; T_s, the demixing temperature; C, crystallization.

III. Method of Morphology Control

Here we briefly describe the thermal history employed here for morphological control. As shown in Figure 2, the cold-pressed starting film specimens Q were rapidly heated to a temperature T_s above T_m of PP in the mixture and held at T_s for various lengths of time $(t - t_s)$ (cf. process a in the figure).[38] The samples subjected to demixing at T_s for the time period $(t - t_s)$ were then allowed to crystallize either by rapid quenching below T_m (athermal crystallization) or by rapid quenching to a given temperature T_c for the isothermal crystallization (cf. process b in the figure).

The rapid temperature rise to T_s was produced by inserting the film specimen Q into the hot stage precontrolled at T_s. The time t_s is the time required for the film specimen to achieve the equilibrium temperature T_s and was measured to be about 20–30 s with a thermocouple embedded in the sample. Consequently one can neglect the thermal history occurring during the time period t_s for time scale $t - t_s > 100$ s. It should be noted that the melting temperature T_m applies to the mixture with the parrticular composition of PP (F_{PP}) employed in this work. The horizontal dashed–dot line in the figure does not mean the composition dependence of T_m but represents T_m at the particular composition used.

The mixture was shown to be very immiscible at all temperatures[37] where the polymers do not significantly degrade thermally. Thus the system undergoes demixing. The demixing was found to occur according to spinodal decomposition inside the spinodal phase boundary, as shown by the broken line in Figure 2. The phase diagram in Figure 2 is just a schematic illustration but does not have any quantitative significance. It is used to indicate that the mixture is thermodynamically unstable at all temperatures where the polymers are thermally stable. It is conceivable that the mixture may not have an UCST (upper critical solution temperature) but rather has a "tree-trunk" diagram[32] or "hour-glass"-shaped diagram.

In this work morphology of the samples was controlled by quenching the film specimens, after they had been subjected to isothermal demixing at temperatures T_s for the time periods of $(t - t_s)$, into ice water. The temperatures T_s studied were 170, 200, and 250 °C, and the time periods employed are typically up to $t - t_s \simeq 10^4$ s. The L–L demixing occurs at T_s and the crystallization into spherulite morphology occurs during the quenching into ice water.

IV. Results and Discussion

1. Liquid–Liquid (L–L) Phase Separation: Demixing Above T_m. We first present the demixing of the system in the liquid state above T_m. Figure 3 shows a typical time evolution of the polarized component of scattered light (V_V) at 250 °C. The time $(t - t_s)$ increases from 0 to 7000 s sucessively from the patterns a to j. Note that the angle mark was changed between the upper and lower rows.

The scattering patterns show "ring-scattering" with a scattering maximum at θ_{max} or at scattering vector q_m

$$q_m = (4\pi/\lambda) \sin (\theta_{max}/2) \quad (1)$$

where λ is the wavelength of light in the medium. The maximum shifts toward smaller angles or smaller scattering vectors $q = (4\pi/\lambda) \sin (\theta/2)$. This indicates that the demixing in the thermodynamically unstable liquid state involves formation of periodic concentration fluctuations with the wavelengths Λ_m that increase with time.

A similar trend is also shown in Figure 4 for the isothermal time-evolution of V_V scattering at 170 °C. The absolute values and growth rate of Λ_m are, however, different from those at 250 °C. The wavenumber of growing fluctuations is defined by

$$q_m(t) = 2\pi/\Lambda_m(t) \quad \text{(in real space)} \quad (2)$$

It should be noted that the Fourier component of the fluctuations having the wavenumber q_m given by eq 2 gives rise to the scttering maximum at the scattering vector q_m given by eq 1. Consequently the fluctuations with the wavenumber $q_m(t)$ in real space can be directly estimated from the scattering intensity at the scattering vector q_m in reciprocal space.

In Figure 5 are summarized the changes of the wavenumbers q of the fluctuations with time at the three temperatures 170, 200, and 250 °C. At this stage one should refer only to the data shown by the filled marks. At all temperatures q_m decreases with time as a consequence of various coarsening mechanisms occurring in the late stage of the spinodal decomposition.[17-29] The time dependence of q_m is conventionally expressed as a power law

$$q_m \sim (t - t_s)^{-\alpha} \quad (3)$$

In the time scale covered in this experiment, the data show

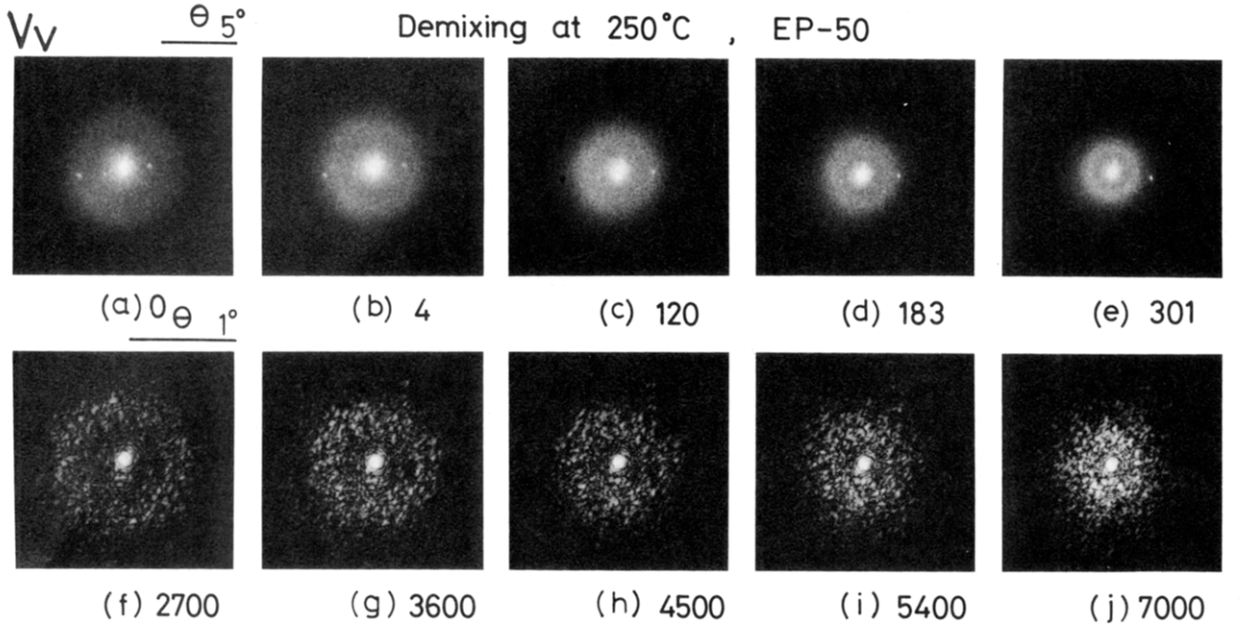

Figure 3. Time evolution of V_V scattering patterns in the isothermal demixing at 250 °C. The time $(t - t_s)$ in seconds after reaching 250 °C is as follows: (a) 0, (b) 4, (c) 120, (d) 183, (e) 301, (f) 2700, (g) 3600, (h) 4500, (i) 5400, and (j) 7000.

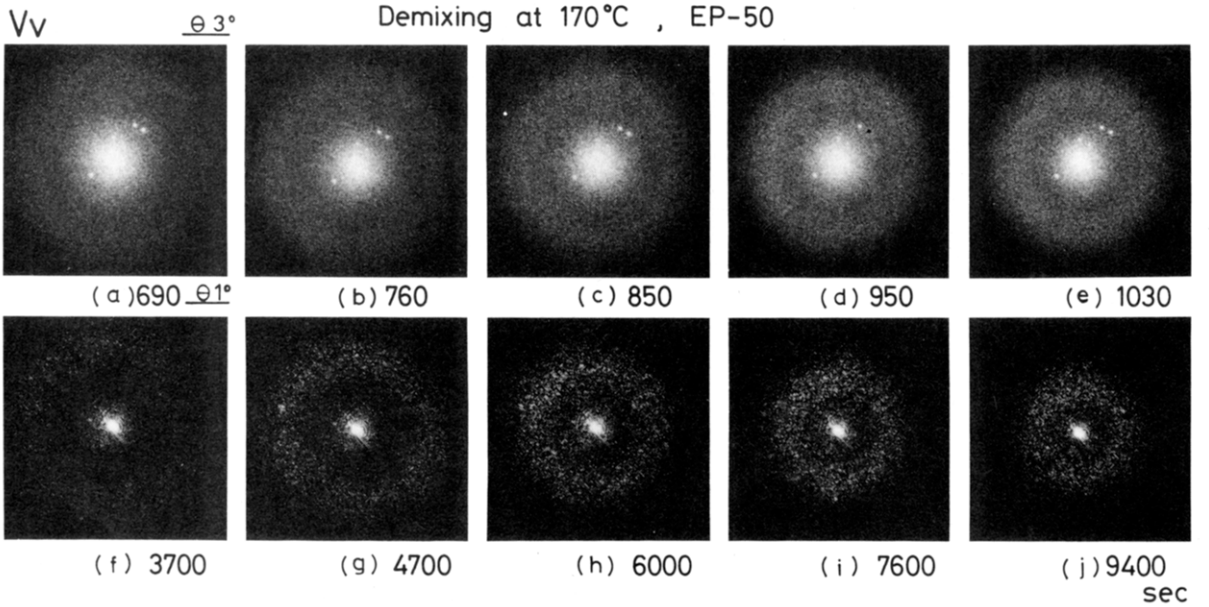

Figure 4. Time evolution of V_V scattering patterns in the isothermal demixing at 170 °C. The time $(t - t_s)$ in seconds after reaching 170 °C is as follows: (a) 690, (b) 760, (c) 850, (d) 950, (e) 1030, (f) 3700, (g) 4700, (h) 6000, (i) 7600, and (j) 9400.

that α is not constant and changes from $^1/_3$ to $^2/_3$. This variation of α with time was reported both theoretically[18,21] and experimentally[24,25,28,29] when q_m was observed over a wide time scale. The value is expected eventually to reach unity, but this limiting value was not attained in the time scale covered in our experiments.

The behavior of q_m at different temperatures fall onto a single master curve if q_m and $t - t_s$ are rescaled by using the reduced parameters Q_m and τ as defined below[33]

$$Q_m \equiv q_m(t)/q_m(t = 0) \quad (4)$$

$$\tau \equiv (t - t_s)/t_c \quad (5)$$

where t_c is a characteristic time given by

$$t_c \equiv \xi^2/D_{app} \quad (6)$$

The quantities ξ and D_{app} are respectively the correlation length and apparent diffusivity in the system at given temperatures before demixing takes place. The quantities

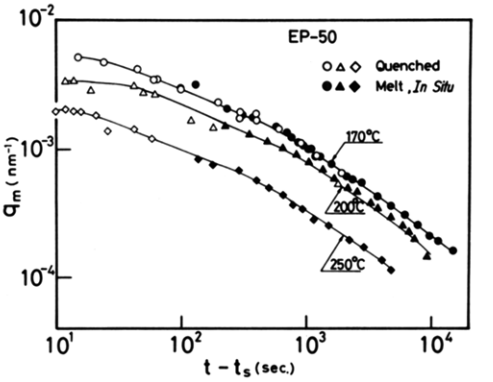

Figure 5. Variation of the wavenumber q_m of the dominant fluctuations with time during the isothermal demixing at 170, 200, and 250 °C. The data shown by filled symbols were obtained in situ at given temperatures but those shown by open symbols were obtained after quenching the mixtures into ice water.

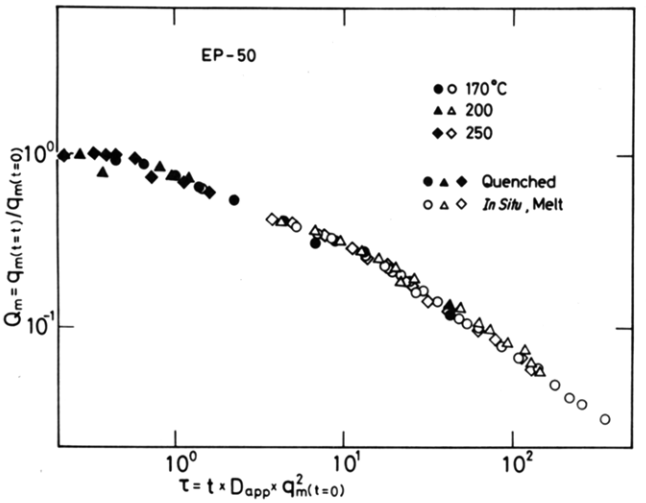

Figure 6. Reduced plot on the reduced wavenumber Q_m and reduced time for the isothermal demixing at 170, 200, and 250 °C. The filled symbols are the Q_m's measured after quenching into ice water, while the open symbols are those measured in situ above T_m.

ξ and D_{app} can be estimated experimentally by analyzing the early stage of spinodal decomposition where the linearized theory of Cahn is valid or at least may be used to a good approximation. In this work ξ and D_{app} at given temperatures were measured according to the method described above[25] and as will be described in detail elsewhere.[2]

$$\xi = 1/q_m(t = 0) \tag{7}$$

$$D_{app} = R(q)/q^2|_{q=0} \tag{8}$$

The quantity $R(q)$ is the growth rate of a particular Fourier component of fluctuations with the wavenumber q. Rigorous determinations of ξ and D_{app} were difficult because of the rapidity of the spinodal decomposition, which makes the time scale of observation quite short. We nevertheless attempted to construct a reduced plot to show qualitatively the general tendency.

Figure 6 shows a reduced plot of Q_m vs τ, indicating qualitatively that the time evolution of the fluctuations at various temperatures occurs according to a common mechanism. Thus the behavior of q_m at 250 °C, for example, corresponds to the behavior of q_m at 170 °C at a later stage. If the reduced plot had true universality for a range of composition of PP/EPR, one could predict $q_m(t)$ at a given temperature from the values $q_m(t=0)$ and D_{app}. Hence one can control the size of periodic concentration fluctuations. Furthermore, one can generally construct a scaling relationship between the reduced scattered intensity and reduced time, which would then allow one to control or predict the amplitude of the fluctuations. One may also predict the values $q_m(t=0)$ and D_{app} at a given temperature from fundamental molecular parameters[10,13] by using scaling relationships.

2. Spherulitic Crystallization and Conservation of "Memory" of Demixed Structure in Liquid State. As mentioned earlier, specimens subjected to demixing to a predesigned stage in the liquid state above T_m were crystallized by rapid quenching into ice water. The supermolecular structure in the quenched film was investigated by studying polarized and depolarized components of small-angle light scattering.

Figure 7 shows typical H_V (upper row) and V_V (lower row) light scattering patterns for films subjected to the demixing at 170 °C for 1 min (a and e), 3 min (b and f), 5 min (c and g) and 10 min (d and h) followed by quenching into ice water. All the films show the clover-leaf H_V scattering patterns typical of spherulites. From the angular position of the scattering maximum $q_{max,s}$ one can determine an average spherulite size[34]

$$(4\pi/\lambda)R_s \sin(\theta_{max,s}/2) = 4.1 \tag{9}$$

The V_V scattering patterns are of two kinds: (i) a pattern at small scattering angles elongated parallel to the vertical direction with a twofold symmetry, and (ii) a

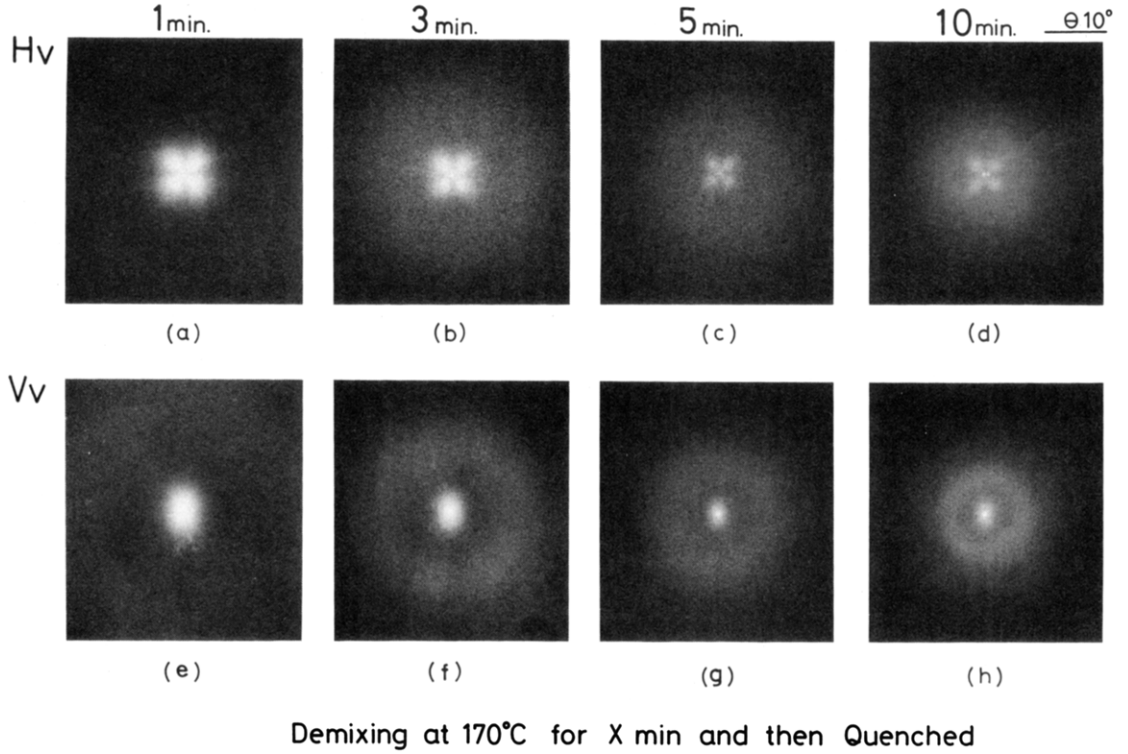

Figure 7. Typical H_V (upper row) and V_V (lower row) light scattering patterns for the films subjected to the demixing at 170 °C for 1 min (a and e), 3 min (b and f), 5 min (c and g), and 10 min (d and h) followed by quenching into ice water.

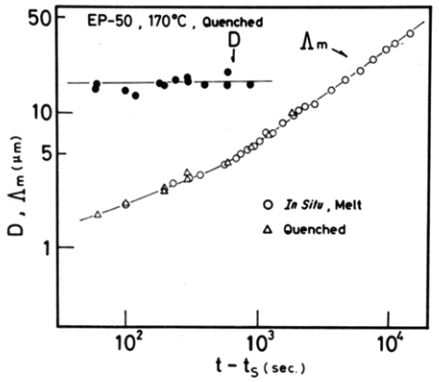

Figure 8. Spherulite diameter D and wavelength Λ_m of the concentration fluctuations built in by the liquid–liquid phase separation for the specimens first demixed at 170 °C for various time periods ($t - t_s$) and then followed by quenching into ice water. The open circles are the Λ_m's measured in situ at 170 °C but the open triangles are those measured after the quenching.

pattern at large scattering having the "ring" appearance without azimuthal angle dependence. The "ring scattering" was found to have the maximum intensity at exactly the same scattering angle, $\theta_{max,l}$ as the ring scattering found in the samples demixed for corresponding period of times at 170 °C. Thus the spacing Λ_m developed in the liquid state does not change during the rapid crystallization process caused by quenching into ice water. For a given specimen, the angle $\theta_{max,l}$ is much larger than the angle $\theta_{max,s}$, indicating that the spacing Λ_m is smaller than the average spherulite radius R_s. The V_V scattering pattern at small angles should then correspond to the spherulitic scattering. From the patterns shown in Figure 7, the values D (=$2R_s$, average diameter of the spherulite) and Λ_m were determined, and the results are plotted in Figure 8 as a function of the time ($t - t_s$) of the isothermal demixing at 170 °C. The results indicate that the average diameter of the spherulites developed in the rapid crystallization process is independent of Λ_m or of the time spent for demixing above T_m. However, the spacing Λ_m depends on ($t - t_s$), i.e., on the memory of L–L phase separation. The data points shown by triangles are the spacing Λ_m observed for the quenched samples, while those shown by open circles are the spacing Λ_m measured in situ above the melting temperature, i.e., the Λ_m's before quenching. It is seen clearly that the *memory of L–L demixing is conserved* during the rapid crystallization process.

The conservation of the memory of the demixing above T_m during the rapid crystallization process is also clearly indicated in Figure 5 where the q_m values measured for the quenched films (open symbols) fall onto those measured in the liquid state (filled symbols). The conservation of memory is also shown in the master curve (Figure 6), where the data obtained for the quenched samples (filled circles, triangles, and diamonds) and those obtained for the liquid state (open circles, triangles, and diamonds) fall onto the same master curve.

3. Effect of Annealing: Space-Filling Spherulites Having "Memory of L–L Demixing" as an Internal Structure. In this section we consider whether the memory of the L–L demixing is conserved within the spherulites or in the interstitial space between the spherulites. In order to clarify this point we annealed the quenched and as-prepared films at various temperatures below T_m for various periods of time.

A typical result is shown in Figure 9. Figure 9, parts a and c, represent respectively H_V and V_V scattering patterns for the quenched and as-prepared films, the

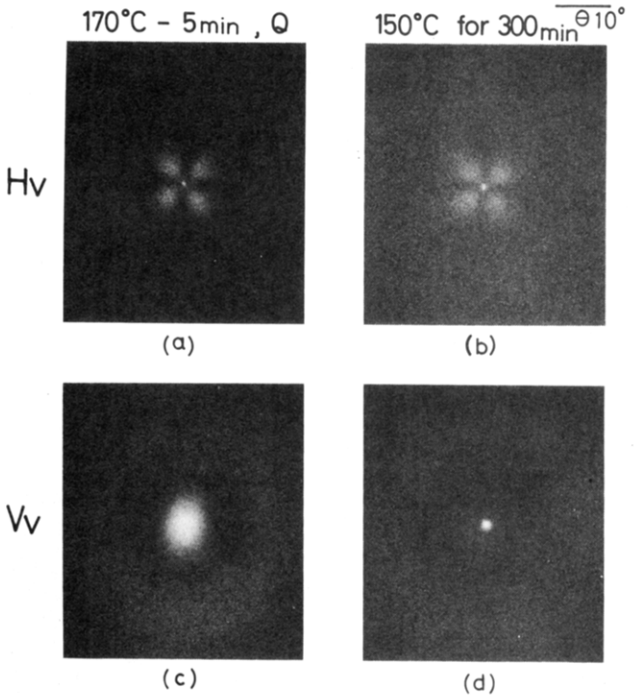

Figure 9. Effect of annealing the quenched films at 150 °C for 300 min on the spherulite size and its internal "structure memory". Upper (a and b) and lower (c and d) patterns correspond to H_V and V_V scattering patterns, respectively. The patterns a and c are those for the quenched films, while b and d are those for the annealed films. The quenched films were obtained by demixing at 170 °C for 5 min and by subsequent quenching the film into ice water.

system being subjected to demixing at 170 °C for 5 min. Figure 9, parts b and d, represent the corresponding scattering patterns from the same film subjected to a further annealing at 150 °C for 300 min.

Outstanding features of the effects of annealing are that $\theta_{max,s}$ and $\theta_{max,l}$ are essentially unaltered by the annealing process. This indicates that the spherulite size D and R_s and the memory of L–L spacing Λ_m do not change with the annealing. It is believed that the size of the spherulite is conserved because the spherulites developed during the rapid quenching impinge on each other and fill the whole sample space. Further annealing below T_m, e.g., at 150 °C, would involve no further growth of the spherulite size but involve only secondary crystallization within the spherulites, leading to a higher crystallinity and higher scattering power, as seen from the enhanced multiple scattering in the annealed film.

The fact that the quenched films contain volume-filling spherulites clearly indicates that the L–L *demixing memory is conserved within the spherulites* rather than the interspherulitic regions. The memory built in the spherulites is essentially conserved during the annealing, indicating that the crystallization or presence of crystallinity prevents further coarsening of the memory of the L–L demixing.

4. Mechanism of Crystallization. The experimental evidence and the discussions in sections IV-1–IV-3 help to visualize the mechanism of the crystallization involved by the rapid quenching from the demixed state. The crystallization would follow essentially the same trend as the one specified by the *solidification* concept proposed by Fischer and his co-workers:[35] the crystallization and spherulitic crystallization occur through the phases or domains enriched in PP without involving segregation of EPR from the crystallization front or growing front of PP

crystallites, i.e., without involving global rearrangements of PP and EPR during crystallization ("diffusion-limited growth" of crystallites).

It is important to note that for the given crystallization conditions employed in the present work the rate of crystallization is much faster than the rate of global diffusion of polymers that would be required for the segregation of EPR out of the growing front of PP crystallites. This may be the fundamental reason for the conservation of the L–L demixing memory. The spatial variation of the concentration of crystallizable PP would cause the spatial variation of the melting temperature, the supercooling, the rate of crystallization of PP, and hence the spatial variation of local crystallinity. This spatial variation is superposed on the fine spatial variation of the local crystallinity produced by stacked lamellae along the direction normal to the lamellar interfaces.

V. Concluding Remarks

The role of L–L demixing on the morphology produced by subsequent crystallization is discussed. For a rapid crystallization process, the L–L demixing memory was found to be conserved and built into the volume-filling spherulites. The size of the spherulites and the spacing of the L–L demixing memory were also found to be conserved during further annealing of the as-prepared quenched films at temperatures below T_m.

Further work is obviously desirable on (i) the control of spherulite size, (ii) the criterion required for the conservation of the L–L memory of demixing when the crystallization is conducted slowly at higher temperatures, (iii) quantitative kinetic studies of growth of spherulites, and (iv) morpholigical studies of the crystalline superstructure. Some of these aspects will be presented in a subsequent paper.[36]

Acknowledgment. We are grateful to Professor W. H. Stockmayer for critical reviews.

Registry No. PP, 9003-07-0; EPR, 9010-79-1.

References and Notes

(1) See, for example: (a) Nicolis, G.; Prigogine, I. *Self-Organization in Nonequilibrium Systems—from Dissipative Structures to Order through Fluctuations*; Wiley: New York, 1977. (b) Haken, H. *Synergetics—An Introduction, Nonequilibrium Phase Transitions and Self-Organization in Physics, Chemistry and Biology*, Springer-Verlag: Berlin, 1978.
(2) Tanaka, K.; Hashimoto, T.; Kawai, H., to be submitted.
(3) Cahn, J. W. *J. Chem. Phys.* **1945**, *42*, 93.
(4) Cook, H. E. *Acta Metall.* **1970**, *18*, 297.
(5) Van Aartsen, J. J. *Eur. Polym. J.* **1970**, *6*, 919.
(6) de Gennes, P.-G. *J. Chem. Phys.* **1980**, *72*, 4756.
(7) Binder, K. *J. Chem. Phys.* **1983**, *79*, 6387.
(8) Nishi, T.; Wang, T. T.; Kwei, T. K. *Macromolecules* **1975**, *8*, 227.
(9) Nojima, S.; Tsutsumi, K.; Nose, T. *Polym. J. (Tokyo)* **1982**, *14*, 225.
(10) Hashimoto, T.; Kumaki, J.; Kawai, H. *Macromolecules* **1983**, *16*, 641.
(11) Snyder, H. L.; Meakin, P.; Reich, S. *Macromolecules* **1983**, *16*, 757.
(12) Hashimoto, T.; Sasaki, K.; Kawai, H. *Macromolecules* **1984**, *17*, 2812.
(13) Sasaki, K.; Hashimoto, T. *Macromolecules* **1984**, *17*, 2818.
(14) Izumitani, T.; Hashimoto, T. *J. Chem. Phys.* **1985**, *83*, 3694.
(15) Russell, T. P.; Hadziioannou, G.; Warburton, W. K. *Macromolecules* **1985**, *18*, 78.
(16) Hashimoto, T. In *Current Topics in Polymer Science—Polymer Physics*; Utracki, L. A., Ed., Hanser: Munich, 1986; Vol. 2.
(17) Langer, J. S.; Bar-on, M.; Miller, H. S. *Phys. Rev. A.* **1975**, *11*, 1417.
(18) Kawasaki, K.; Ohta, T. *Prog. Theor. Phys.* **1978**, *59*, 362.
(19) Binder, K.; Stauffer, D. *Phys. Rev. Lett.* **1974**, *33*, 1006.
(20) Lifshitz, I. M.; Slyozov, V. V. *J. Phys. Chem. Solids* **1961**, *19*, 35.
(21) Furukawa, H. *Prog. Theor. Phys.* **1978**, *59*, 1072; *Phys. Rev. Lett.* **1979**, *43*, 136.
(22) Siggia, E. D. *Phys. Rev. A* **1979**, *20*, 595.
(23) Nojima, S.; Ohyama, Y.; Yamaguchi, M.; Nose, T. *Polym. J. (Tokyo)* **1982**, *14*, 907.
(24) Kuwahara, N.; Tachikawa, M.; Hamano, K.; Kenmochi, Y. *Phys. Rev. A* **1982**, *25*, 3349.
(25) Snyder, H. L.; Meakin, P. *J. Chem. Phys.* **1983**, *79*, 5588.
(26) Komura, S.; Osamura, K.; Fuji, H.; Takeda, T. *Phys. Rev. B: Condens. Matter.* **1985**, *31*, 1278.
(27) Shimizu, N.; Itakura, M.; Hashimoto, T., to be submitted to *Macromolecules*.
(28) Hashimoto, T.; Itakura, M.; Hasegawa, H. *Polym. Prepr. Jpn. Soc. Polym. Sci. Jpn.* **1985**, *34*, 2773; Japan–US Polymer Symposium Preprints, Oct 29–Nov 1, 1985, Kyoto, Japan; p 15.
(29) Yang, H.; Shibayama, M.; Stein, R. S.; Shimizu, N.; Hashimoto, T. *Macromolecules*, in press.
(30) Suehiro, S.; Takebe, T.; Hashimoto, T.; Izumitani, T. *Polym. Prepr. Jpn., Soc. Polym. Sci. Jpn.* **1984**, *33*, 2739.
(31) Suehiro, S.; Takebe, T.; Izumitani, T.; Hashimoto, T.; Japan–US Polymer Symposium Preprints, Oct 29–Nov 1, 1985, Kyoto, Japan; p 322.
(32) Sanchez, I. C.; Lacombe, R. H. *J. Phys. Chem.* **1976**, *80*, 2352, 2568.
(33) Chou, C.; Goldburg, W. I. *Phys. Rev. A* **1979**, *20*, 2105.
(34) Stein, R. S.; Rhodes, M. B. *J. Appl. Phys.* **1960**, *31*, 1873.
(35) Stamm, M.; Fischer, E. W.; Dettenmaier, M.; Convert, P. *Faraday Discuss. Chem. Soc.* **1979**, *68*, 263.
(36) Inaba, N.; Sato, K.; Suzuki, S.; Hashimoto, T., to be submitted to Macromolecules, part 2 of this series.
(37) The spinodal temperature T_s was estimated to be about 300 °C from the dynamic studies in the early stage of spinodal decomposition[2] where the dominant wavenumber of the fluctuations in the earl stage q_m was measured as a function of temperautre T, and T_s was determined as T which satisfies $q_m^2(T=T_s) = 0$ by extrapolating the observed linear relationship between q_m^2 and T (satisfying $q_m(T)^2 \sim |T_s - T|$ with a good approximation, at least) toward $q_m^2 = 0$. Thus, the spinodal temperature for this particular system does not exist in an achievable temperature range where thermal degradation does not occur and hence cannot be directly determined by conventional methods. However, it is conceivable that T_s may exist in the achievable temperature range for other mixtures of PP and EPR with molecular weights comparable to the mixtures to be studied here, since T depends upon the ethylene content of EPR, its sequence distribution, the tacticity of propylene sequences, and the fraction of PP (F_{pp}).
(38) The demixing kinetics of the films prepared by precipitation from the mutual solvent are expected to depend generally upon precipitation conditions. A particular precipitation condition (as described in the text) was employed in this study, and the effect of the precipitation conditions on the kinetics was not explored. It is expected, however, that the precipitation conditions will not dramatically modify the conclusions obtained in this paper.